Experimental study of the effects of the long chimney of a closed tonehole on the sound of a bassoon

Augustin Ernoult, Timo Grothe

Experimental study of the effects of the long chimney of a closed tonehole on the sound of a bassoon

Augustin Ernoult[1, a] and Timo Grothe[2]

[1] *Project-team Makutu, Inria Bordeaux Sud-Ouest, Université de Pau et des Pays de l'Adour, E2S UPPA, CNRS, 200 avenue de la vieille Tour, 33405 Talence Cedex, France*

[2] *Erich Thienhaus Institut - Hochschule für Musik Detmold, Neustadt 22 D - 32756 Detmold, Germany*

(Dated: 17 February 2023)

The bassoon has side holes a few tens of millimeters long, much longer than in other woodwinds. When they are closed, the "quarter-wave" resonances of these "chimneys" create short circuits in parallel with the bore. At these resonance frequencies, near 2 kHz –within the sensitive range of hearing– it is expected that the waves will not propagate beyond the chimney, affecting both the input impedance and the radiated sound. Using parametric studies with varying chimney lengths, these effects on impedance and radiated sound are measured for a French bassoon and a simplified conical model instrument. The effects are clear on the model instrument, especially when several chimneys have equal length. For the bassoon, the passive filter effect remains, but its importance on the sound is blurred due to changes in the oscillation regime and in the directivity, as simulations confirmed. The effect is audible under laboratory conditions, but in the same order of magnitude as the spatial level variations due to the directivity. It is therefore unlikely that the difference in timbre between the French and the German bassoon is mainly due to longer tone hole chimneys.

Pages: 1–14

I. INTRODUCTION

From a mechanical point of view, a wind instrument is composed of two parts: the oscillator (reed, lips or jet) generating the acoustic vibration, and the body which has two acoustic functions. The wall of the instrument delimits an air column that vibrates and, through the resonance phenomena, selects the frequency at which the instrument sounds. This role of a resonator is generally associated with the acoustic input impedance (Chaigne and Kergomard, 2016, Chap.7). The second function, less studied, is sound radiation. The body influences how each frequency component of the sound is radiated into the room in terms of magnitude and directivity and so affects the frequency content of the perceived sound. Some recent studies propose to use transfer functions between acoustic quantities at the reed position and into the room to characterize this radiator function (Grothe and Amengual Garí, 2019; Petersen *et al.*, 2022).

In some wind instruments (mostly woodwinds) side holes are drilled through the wall of the body, allowing the pitch of the sound to change. At low frequency, when a hole is open, it imposes a node of pressure at its location, which has the effect of reducing the effective length of the body of the instrument and to increase its frequency of resonance. When a hole is closed, its chimney pipe can, at low frequency, be seen as additional volume (Chaigne and Kergomard, 2016, Chap.7.7.5.2), slightly elongating the effective length (Debut *et al.*, 2005).

However, the chimneys can also be seen as side branches of the main bore pipe with their own frequencies of resonance. At these frequencies, the acoustic wave is completely reflected at the side-branch location as described by Pierce (1989, Chap.7.4, Chap.7.7) for the case of a side Helmholtz resonator. As the wave does not propagate downstream in the main duct, the branch acts as an acoustic "notch filter". For a closed cylindrical side-branch of length L, the notch occurs at a frequency corresponding to a wavelength $\lambda \approx 4L$, which led to the term "quarter wavelength resonator" (Field and Fricke, 1998). This principle can be used to design a passive reactive muffler, with an array of side-branches of different lengths as proposed by Tang (2012) in air conditioning systems.

This effect also influences the behavior and the radiated sound of wind instruments. In most of them the chimneys are relatively short ($L < 7$ mm), giving high characteristic frequencies ($f > 10$ kHz). However, the bassoon has very long chimneys, sometimes longer than 40 mm ($f \approx 2$ kHz). This is a peculiarity of the bassoon, related to its length: To place the holes at appropriate positions in the air column, and to still be able to close them with the fingers, the corresponding holes are drilled obliquely into the body part named the "wing joint" on

[a] augustin.ernoult@inria.fr

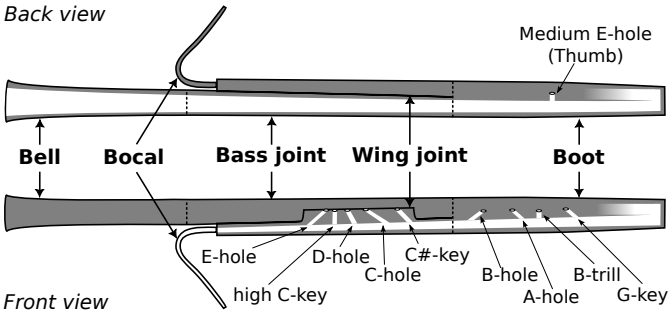

FIG. 1. Sketch of a French bassoon (back and front view). For readability, only half of the air column (in white) is plotted on each view (between the reed and the boot bend on the front view, and between the boot bend and the bell on the back view), and only the holes with the longest chimneys are represented.

account of its locally thickened wall (Fig. 1). These long chimneys have been conserved during the evolution of the instrument and are still present in the two types of bassoons mainly used today: the French and the German. For the latter the chimneys are about 5 mm shorter on average (Kergomard and Heinrich, 1975; Nederveen, 1998). It has been suggested that that the long closed chimneys contribute to the specific sound color of the instrument and are one of the reasons for the low success of bassoons with short chimneys built during the 19th century (Kergomard and Heinrich, 1975).

Following acoustic arguments similar to the ones evoked previously, J. Kergomard suggests that these long chimney pipes, some of which are closed for the majority of the notes, induce a notch near 2 kHz in the radiated spectrum of the bassoon (Kergomard and Heinrich, 1975) (Chaigne and Kergomard, 2016, Chap.7.7.5, p.374). More recently, Petersen *et al.* (2021), in a study on the "tone hole lattice" of the bassoon, advance and complete this study by an up-to-date theoretical approach. The two studies suggest that this phenomenon is one explanation for the timbre difference between French and German bassoons.

However, in these two studies, the experimental data provided are purely qualitative and the notch is quite difficult to observe. Furthermore no parametric study demonstrates the relationship between the length of the long chimney and this slight notch. Indeed, in musical instruments, the acoustic source does not provide the same amount of energy at all frequencies. For a conical instrument, the spectrum of the pressure at the reed location resembles the shape of a *sinc* function (Kergomard *et al.*, 2019). It is then difficult to distinguish if a notch in the external sound spectrum is due to a lack of energy at the reed or a muffling effect by the chimneys. Furthermore, the sound energy mainly decreases with the frequency. The range from 2 kHz, where the phenomenon occurs, corresponds to about the 10^{th} harmonic in the medium register. Here the partials' levels are already low (Petersen *et al.*, 2021). The alteration could be inoperative or imperceptible. Finally, due to the coupling between air-column and reed, the modification of the radiated spectrum by the long chimneys can have two origins. The first possibility relates to the resonator function: the reed motion is affected by the alteration of the input impedance; the second possibility relates to the radiator function: only the radiation efficiency of each component is altered. Of course, both functions may also simultaneously affect the spectrum.

The aim of this study is to clarify how the presence of a long chimney pipe affects the radiated sound of the bassoon. The main goal is to identify and quantify the modification of the radiated spectrum by the presence of long closed chimney pipes and to correlate this effect to their length. A secondary objective is to distinguish whether this modification is a consequence of an alteration of the reed motion or simply a passive acoustic filter effect. Finally, gives some information about the potential perceptual importance of this phenomenon for bassoon timbre.

As a musician is able to adapt to his/her control parameters to compensate the effect of a geometric change on the sound (Fabre *et al.*, 2019), an artificial mouth is used. This allows to focus on the acoustic effect of this modification. Two instruments, in which the length of the chimneys can be modified, are thus played: a French bassoon and a simplified instrument with three chimneys. As it is difficult to study experimentally the behavior of the reed, simulations are carried out in parallel with these measurements. These tools allow the study of the modification of the external sound and the pressure in the reed, when the chimneys' length are varied, while all other parameters are kept constant.

In Section II, the instruments studied are presented. The experimental devices (the impedance sensor and the artificial mouth), and the signal processing used are then briefly described. This "material and methods" section finishes with the presentation of the models used to compute the impedance and the sound synthesis. Section III presents the effect of the long chimneys on the input impedance, the radiated spectrum and the reed pressure spectrum for the two measured instruments and the simulation. These observations are then discussed in Section IV and compared to other sources of the sound spectrum modification. Finally, the conclusions of this study are presented in Section V.

II. MATERIAL AND METHODS

A. Instruments

The bassoon studied here is a Buffet Crampon French Bassoon from 1903. Its entire geometry has been measured with split ball probes (Diatest, Darmstadt, Germany), allowing measurement of diameters with an accuracy about 0.1 mm, and a caliper. Specific attention has been given to the side hole dimension. The dimensions of the nine longest holes are shown in Table I [1].

name	distance [mm]	height [mm]	radius [mm]	f_{chim} [kHz]
E-hole	490	45.5	2.1	1.76
high C-key	507	22.5	2.4	3.33
D-hole	572	37.0	3.0	2.10
C-hole	615	40.5	2.5	1.94
C♯-key	659	33.5	1.7	2.36
B-hole	830	35.5	3.6	2.14
A-hole	903	29.2	3.8	2.53
B-trill	968	28.5	2.9	2.63
G-key	1008	31.5	4.0	2.43

TABLE I. Dimensions of the French bassoon's holes with a chimney pipe longer than 20mm: the commonly used names, the distance to the entrance, the chimney height, the internal radius and the characteristic frequency (Sec. III A).

In this study, a focus is given to an alternative C♯3 fingering of the bassoon (middle range), corresponding to a regular C3 in which the C♯-key is open. Here only the three finger holes with the longest chimneys (E-hole, D-hole and C-hole, see Table I) are closed. Other closed holes in this fingering are some register and sharp/flat key holes, all of which have chimney lengths shorter than 29 mm and are located after open holes. Thin-walled cylindrical tubes with a sliding piston inside were inserted into the chimneys of these three finger holes of the real bassoon. The length of these chimneys can thus be adjusted between 10 mm and 90 mm. The modifications are made keeping the original height offsets between the chimneys (E-hole: +5 mm, D-hole: -3.5 mm, C-hole: 0 mm).

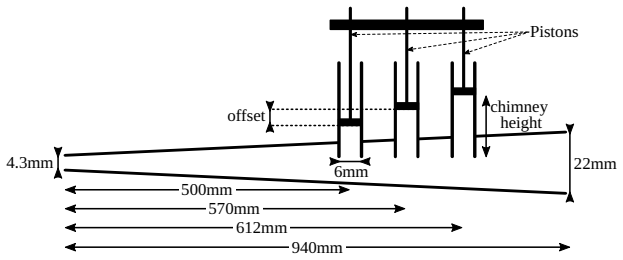

FIG. 2. Sketch of the conical instrument with 3 side holes of adjustable chimney height.

To highlight the effect of the long chimneys, a simplified bassoon is studied: a conical frustum with an input radius equal to that of the bassoon and three side holes of adjustable chimney height (Fig. 2). The output radius and the length of this instrument have been obtained by minimizing the deviation between the simulated impedance of this cone and the measured impedance of the C♯3 fingering of the French Bassoon. The optimization result obtained with the software Openwind (Ernoult *et al.*, 2021) is a cone with an input radius 2.15 mm, output radius 11 mm and 940 mm length. It has been built by coiling a gel filter sheet, with a wall thickness of about half of a millimeter, such that standard bassoon reeds can be plugged into it. The three holes have an internal radius of 3 mm and are located at 500 mm, 570 mm and 612 mm from the entrance of the cone which correspond approximately to the locations of the finger holes in the bassoon (Tab. I). To validate the manufacturing process, the input impedance of the simplified instrument has been measured and compared to simulations (see sections II B 1 and II C 1). Unlike in the bassoon in which the finger holes are drilled obliquely, the three chimneys are parallel. This gives the possibility to hitch the three pistons together (with or without offset) and adjust the length of the three chimneys simultaneously and continuously during the experiments in the range between 0 and 100 mm. Two configurations are measured: a) no offset, the 3 chimneys have the same length; b) offsets of -5 mm, 0 mm and 5 mm, giving three different chimney lengths with deviations of the same order of magnitude as for the bassoon.

B. Experimental set-up and signal processing

Mainly two experimental set-ups are used in this study: an impedance sensor and an artificial mouth.

1. Impedance sensor

The impedance sensor is an adaptation of the Two Microphone Three Calibration method (Gibiat and Laloë, 1990). It has been designed especially for instruments with small input radius (oboe or bassoon) (Eddy, 2016). The probe has an internal radius of 2 mm and is equipped by four microphones allowing the measurement of the impedance from 20 Hz to 5 kHz with good accuracy. The measured microphone signals are analyzed following the approach proposed by Dickens *et al.* (2007) to compute the input impedance.

2. Artificial mouth

The artificial mouth used is the one designed by Grothe (2013, 2015). The lip position, the lip force and the supply pressure can be adjusted. The following parameters are measured: lip force, "mouth cavity" pressure, reed internal pressure, mean flow, and the temperature. For both cone and bassoon, the same plastic reed (Premium Plastic 270M, Conn-Selmer, Elkhardt, USA) is used. The use of micrometer screws to adjust lip position and lip force achieves a very good reproducibility of experiments with the same synthetic reed (Grothe and Baumgart, 2015). The sound is recorded in a recording studio with room dimensions 5.7x5.2x3.6 m^3 and 0.3 s average reverberation time using a measurement microphone (4190, Brüel&Kjær, Nærum, Denmark). For the cone with a single radiating opening, the microphone is placed 1 m from this opening, in line with the main bore axis. For the bassoon, it is placed perpendicular to the

main axis at 1.4 m from the D-hole in the middle of the resonator (Fig. 1). A mobile absorber of 15 cm thickness is placed about 40 cm behind the microphone to avoid strong wall reflections. As the study is focused on the variation of the sound with respect to the length of the chimney, the exact location of the microphone is not crucial as it is kept constant during all measurements. For the bassoon only the C♯3 is played with different chimney length configurations. The lip force and the supply pressure are adjusted to play a C♯3 "in tune" for the shortest chimney lengths. For the cone the artificial mouth parameters are adjusted to produce a stable sound at constant pitch. The fundamental frequency varies by a few percent with the modification of the chimney length, resulting in a mean value of 137 Hz for the bassoon and 130 Hz for the simple cone.

For reed instruments, the same set of parameters can lead to different oscillation regimes depending on the way these values are reached, as illustrated for the saxophone by Colinot *et al.* (2020). Due to this high sensitivity of the produced sound to the artificial mouth parameters, it is necessary to measure one given set of data without shutting down the mouth and within a relatively short amount of time. With the cone, one long recording of 30 seconds is carried out and the chimney lengths are continuously varied during the measurement. During that time, the chimney length is altered back and forth over its whole adjustment range to confirm the stability of the artificial blowing. The chimney pistons are moved together and their relative positions are acquired continuously during the experiment thanks to a draw wire position sensor (SP2, Celesco, Chatsworth, USA). For the bassoon, due to the oblique chimney angles, the chimney lengths need to be adjusted independently at the pistons using a caliper. To accomplish this, we employ a repeated capture scheme, recording one second of steady sound after each length adjustment step. The artificial mouth is not stopped in between each step. The experimenter steps back from the instrument behind a mobile absorber during the recording to avoid disturbance of the directivity pattern. Since each of these measurements is time consuming, length steps of only 10 mm are measured. This reduces the total measurement time and prevents the control parameters from varying too much between steps.

3. Sound signal processing

To estimate the harmonic content of the external sound and the internal reed pressure, a specific signal processing for sustained tones is used: the period-synchronized sampling (Grothe, 2013). After an analysis of zero crossings, the waveform is split into successive periods. Linear interpolation is used to resample each of these periods between zero crossings to ensure that each period is sampled with an integer number of equidistant time steps. The signal energy in each single period is distributed in the frequency domain across components harmonic to the respective f_0. Redistributing these spectra on the continuous time scale leads to a spectrogram with non-equidistant time scale, time-varying frequency resolution and only harmonic components. For the cone experiment with continuous length variation, the spectra are redistributed on a chimney length scale instead of a time scale. This alternative representation readily maps the influence of the chimney length on the spectrum. In the bassoon experiment with discrete chimney length variations, the same processing has been used to preserve comparability. Here, all periods of one capture were averaged in the time domain and the spectrum of this unique period, corresponding to the respective discrete chimney length, is computed.

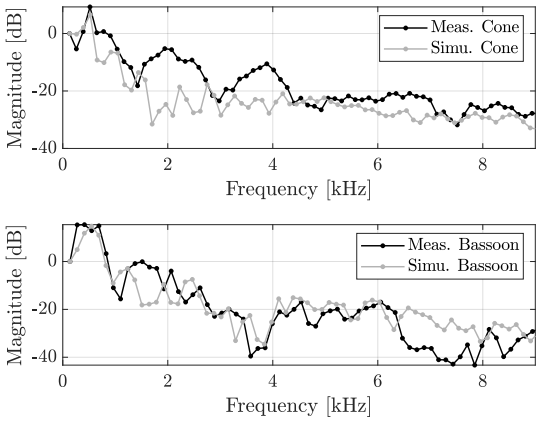

FIG. 3. Magnitude of harmonic components of the external sound averaged for all the chimney length and scaled by the fundamental component magnitude. Top: simple conical instrument measured (black) and simulated (gray); Bottom: French bassoon measured (black) and simulated (gray).

Before looking for the quarter-wavelength-effect, an average spectrum was obtained by averaging the magnitudes of each partial A_i over all chimney heights. These mean spectra $\overline{A_i}$ are plotted, for both instruments, in Figure 3. As expected for conical instrument, the spectra show regular notches (Kergomard *et al.*, 2019), most clearly visible for the simplified instrument (Fig. 3 top, at 1.5 kHz, 3 kHz, etc). This effect is less clear for the bassoon, possibly due to the strong influence of its directivity on a single-point measurement. For both cone and bassoon, the harmonics in the "muffling" frequency range (1.8-3.3 kHz for a French bassoon, see Tab. I) are attenuated by at least 10 dB compared to the strongest partials.

To highlight the variation of the harmonics' magnitudes with chimney length in the rest of the study, only

$$\Delta L_i = 20 \log_{10} \left(\frac{A_i(n)}{\overline{A_i}} \right), \qquad (1)$$

the deviation in decibel of the magnitude of each harmonic component A_i to its mean value over the entire measurement set $\overline{A_i}$ is displayed. The analysis is com-

puted period by period and the variation of the fundamental frequency and harmonic frequencies (within 1% for each measurement) is not represented. For readability reasons, in the rest of the study and in the graphs, each partial is named by its average frequency in kHz.

C. Numerical simulation

All simulations are made with the software Openwind (2022), including the impedance computation and the sound simulation.

1. Input impedance

The body of the instrument is modeled as a network of pipes (main bore and side holes). For a pipe of length ℓ, the acoustic pressure $P(x,\omega)$ and flow $U(x,\omega)$ are computed with the telegrapher's equation, written here in the frequency domain:

$$\begin{cases} \ell Z_v(x,\omega)U_n + \dfrac{dP}{dx} = 0 \\ \ell Y_t(x,\omega)P_n + \dfrac{dU}{dx} = 0 \end{cases} \qquad \forall x \in [0,1], \qquad (2)$$

where Z_v and Y_t are the viscous impedance and thermal admittance modeling the losses (Zwikker and Kosten, 1949) (Chaigne and Kergomard, 2016, Chap.5.5). At the junction between the main bore pipe and a chimney, the relation between the volume flow u_1, u_2, u_3 and the pressure p_1, p_2, p_3 at each pipe end (upstream part, downstream part and chimney) is given by the equation (Ernoult *et al.*, 2021)

$$\begin{aligned} j\omega \begin{pmatrix} m_{11} & m_{12} \\ m_{12} & m_{22} \end{pmatrix} \begin{pmatrix} u_1 \\ -u_2 \end{pmatrix} &= \begin{pmatrix} 1 & 0 & -1 \\ 0 & 1 & -1 \end{pmatrix} \begin{pmatrix} p_1 \\ p_2 \\ p_3 \end{pmatrix} \\ u_1 - u_2 - u_3 &= 0. \end{aligned} \qquad (3)$$

where m_{ij} are acoustic masses (often expressed in equivalent lengths) related to geometry of the junction (Lefebvre and Scavone, 2012). The boot bend of the bassoon is modeled as a straight cone, the length of which is tuned to conserve the volume of the actual geometry.

To compute the impedance, Equations (2) are solved in the frequency domain using 1D finite elements (FEM) for the spatial discretization. A unitary flow is imposed at the entrance for each frequency. In this case, the radiation impedances are computed with the non-causal fit proposed by Silva *et al.* (2009). More technical details on the impedance computation can be found in previous articles (Ernoult *et al.*, 2021; Tournemenne and Chabassier, 2019).

2. Reed-Resonator Interaction

To synthesize the sound of the two instruments it is necessary to solve the telegrapher's equation Eq. (2) in the time domain. In addition to the FEM, an energy-based method is used to discretize the wave equation in time, using a diffusive representation to model the thermo-viscous losses. The scheme used and its implementation are detailed by Thibault and Chabassier (2021). For the radiation conditions, a first order Padé development is used, following for example the work of Rabiner and Schafer (1978).

A tube modeling the wave propagation inside the reed must be added at the entrance of the instrument. The effective geometry of this tube is chosen to be a cylinder having same internal diameter as the output of the actual reed: 5.3 mm. Its length is obtained similarly than the geometry of the conical instrument (Sec. II A), by minimizing the deviation between the simulated impedance of the cylinder and the impedance measured at the output of the reed (for $f \in [100\text{ Hz}, 5\text{ kHz}]$). This gives a length of 45 mm, and a reed equivalent volume of about 1 cm^3.

The equations used to model the double reed are strongly inspired from the work of Bilbao (2009). The numerical schemes used have been refined by Thibault and Chabassier (2020), to be energy preserving. The double reed is described as an oscillator with one degree of freedom, characterized by a set of effective coefficients: the equilibrium height of the reed's channel H_r, the effective width W_r of an area-equivalent, rectangular reed channel with instantaneous height $y(t)$, the effective stiffness K_r, the effective oscillating surface of the reed S_r, the natural frequency ω_r and the quality factor Q_r, completed by the supply pressure p_m. The effective reed channel height $y(t)$ is given by this system of equations:

$$\begin{aligned} \ddot{y} + \tfrac{\omega_r}{Q_r}\dot{y} + \omega_r^2(y - H_r) &= -\tfrac{\omega_r^2}{K_r}\Delta p \\ \Delta p &= p_m - p_{in} \\ u_m &= W_r[y]^+\sqrt{\tfrac{2|\Delta p|}{\rho}}\operatorname{sign}(\Delta p) \\ u_{in} &= u_m - S_r\dot{y} \end{aligned} \qquad (4)$$

where u_{in}, p_{in} are the acoustic flow and pressure at the entrance of the instrument and where $[y]^+$ refers to positive y (when the reed is open). Since the goal of the simulations is to observe how the sound is affected by the long chimney and not necessarily to reproduce the exact waveform, the model is simplified by neglecting the contact force between the reed blades. They can interpenetrate ($y < 0$), in which case the flow is zero. As discussed by Colinot *et al.* (2019), this "ghost reed" simplification influences the sound spectrum by underestimating the absolute magnitude of the high components but not the general behavior of the instrument. In particular, it is assumed that this does not influence the relative variation of the spectrum due to a change of the impedance.

The height H_r, is estimated from a close-up frontal image of the reed inlet. To measure the natural frequency of the reed ω_r and the quality factor Q_r, the reed is plugged on a cylindrical tube in which a loudspeaker injects an acoustic chirp. A laser vibrometer (PDV100, Polytec, Waldbronn, Germany) measures the pressure-induced vibration of the tip of the reed. The frequency at which the response is maximal gives the natural frequency ω_r, and the -3 dB bandwidth gives the quality

p_m	measured	3.58 kPa
u_A	measured	0.79 l/s
p_M	measured	8.76 kPa
H_r	measured	1.0 mm
ω_r	measured	$2\pi \times 1700$ rad/s
Q_r	measured	14.5
W_r	$\frac{u_A}{H_r\sqrt{2p_M/\rho}}$	6.5 mm
K_r	p_M/H_r	8.76 kPa/mm
S_r	tuned	0.75 ; 1.05 cm^2

TABLE II. Values of reed parameters used for sound synthesis. For all parameters the same values have been used for both instruments; except for Sr a tuning was necessary (Bassoon: $S_r = 0.75$ cm^2; conical instrument: $S_r = 1.05$ cm^2).

factor. The measurements show, that in a certain range of lip force the quality factor remains the same.

The measurement of the quasistatic pressure-flow characteristic allows the indirect estimation of the effective width of the reed channel W_r and the effective stiffness K_r. The volume flow is measured with a flow meter and a mass of clay is stuck on the reed blades to avoid oscillations during this measurement which does not affect the quasistatic behavior (Almeida *et al.*, 2007). The pressure p_m is then increased step by step. In quasistatic conditions, Eq. 4 becomes the valve-characteristics of the reed

$$u_m = u_A \left(1 - \frac{\Delta p}{p_M}\right) \sqrt{\frac{\Delta p}{p_M}}, \tag{5}$$

with $p_M = K_r H_r$, the closing pressure and $u_A = W_r H_r \sqrt{2p_M/\rho}$, a characteristic flow. Parameters u_A and p_M are determined by fitting this classical model to experimental data.

These experimental set-ups give access to reed parameters representative of a bassoon-like embouchure. The values chosen for the simulations are indicated in Table II. They are consistent with previous measurements (Grothe, 2015). The effective surface S_r cannot be easily measured. Its value is tuned independently for the bassoon and the simple conical instrument, by trial and error, to obtain about the same fundamental frequency in simulation and measurements (on average, respectively a 6 cent and 18 cent difference in pitch).

The sound simulations are run for different chimney lengths in 1 mm steps for the simple instrument and 5 mm steps for the bassoon. For each configuration a sound simulation of 0.5 s is computed. The mouth pressure increases linearly from 0 Pa to the target supply pressure p_m in 20 ms. The transients are excluded by analyzing only the last 100 ms of each simulation. To study the properties of the source, the effective reed blade distance $y(t)$ as well as the flow rate and the acoustic pressure at the input of the air column are recorded. Their spectrum is processed in a similar way to the bassoon experimental signal (Sec. II B 3) to obtain the variation of the partials with respect to the length of the chimneys.

3. Radiation

The radiation is studied through the total power radiated at each frequency $P_{rad}(\omega)$. It corresponds to the integration of the acoustic intensity over a sphere surrounding the instrument. This quantity excludes the effects of directivity and can be seen as the mean sound spectrum. For the bassoon radiating from multiple source locations (open holes and bell), it is computed as the sum of the power radiated by each opening at each frequency:

$$P_{rad}(\omega) = \sum_{n=1}^{N} P_{rad}^{(n)}(\omega) \tag{6}$$

The power $P_{rad}^{(n)}(\omega)$ radiated at the nth opening is computed from the spectrum of the flow $|U_n(\omega)|$ at this opening in playing conditions as (Chaigne and Kergomard, 2016, Chap.12.3.3, p.642):

$$P_{rad}^{(n)}(\omega) = \frac{1}{2}\Re(Z_{rad})|U_n(\omega)|^2 \approx \frac{\rho}{8\pi c}\omega^2|U_n(\omega)|^2. \tag{7}$$

where $U_n(\omega)$ is the magnitude of the volume velocity at the frequency ω. This is computed from the simulated temporal signal with the same signal processing as the experimental data (Sec. II B 3).

The simulations' spectrum, averaged over all chimney lengths, is compared to that of the measurements in Figure 3. Since the "ghost reed" approximation tends to underestimate the magnitude of the high frequency components, the observed discrepancy between the simulated and measured data is expected. This lack of high frequencies is more pronounced for the simple instrument (Fig. 3, top). For the bassoon (Fig. 3, bottom), an acceptable general agreement is found in the range [2, 6] kHz. In addition, the formants around 0.5 kHz, and the notches around 1 kHz and 3.5 kHz are approximately predicted. Beyond neglecting the contact force, the deviation at low (< 1 kHz) and high frequencies (> 6 kHz) can also be a consequence of the use of a single microphone in the experiment data combined with the spatial distribution of the acoustic fields (e.g., directivity of the instrument, room reflections, external tone-holes interaction, etc). In presented simulations, all these effects do not occur due to the observation of the total radiated power.

However, since the analysis is focused on the relative variation in harmonic content due to the change in chimney length, these discrepancies between simulations and measurements are not critical here: the goal is simply to validate whether the simulations are able to predict how long chimneys affect the radiated sound and not whether they correctly predict the sound, in absolute terms.

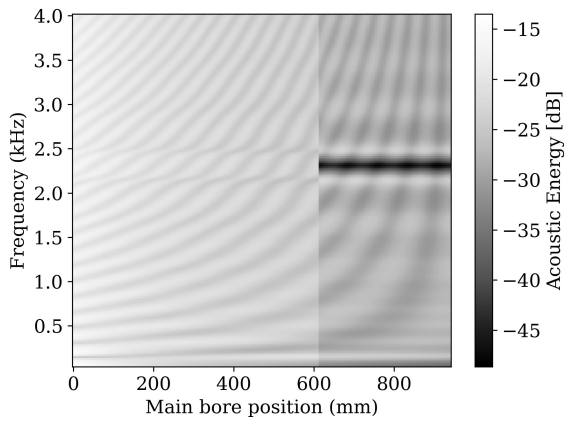

FIG. 4. Simulation of the acoustic energy distribution along the main bore of the simplified instrument with the third chimney pipe set to 35mm and the two other to 0. The energy is scaled by the mean energy in the instrument for each frequency.

III. RESULTS

A. Effect on the impedance

As already discussed by Petersen *et al.* (2021), the presence of long chimneys affects the wave propagation along the main bore of the instrument at specific frequencies. The chimney pipe acts as a muffler which "traps" acoustic energy at its characteristic frequencies, and dissipates it through visco-thermal effects. To illustrate how this affects the input impedance of the instrument, the wave propagation into the simplified cone with only one closed chimney (located at 612 mm with a length of 35 mm, see Fig. 2) is simulated.

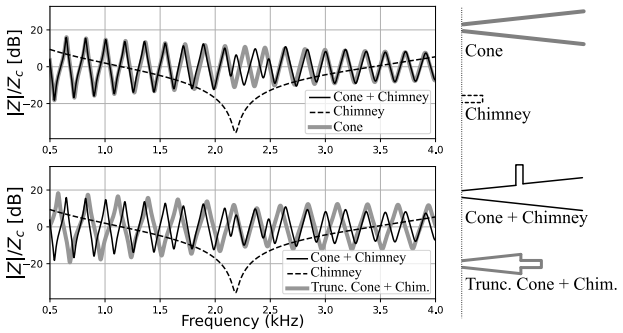

FIG. 5. Input impedance of the simplified instrument with one closed long chimney (thin black line) and of the closed chimney alone (thin dashed line). Top: input impedance of the cone without side hole (thick grey line). Bottom: input impedance of the cone truncated at the hole location and extended by the closed chimney (thick grey line).

The acoustic energy distribution along the main bore for each frequency is represented in Fig. 4. The energy $E(f,x)$ at the frequency f and the location x is defined as: $E(f,x) = \frac{1}{2}\Re(Y_t(f,x))|p(f,x)|^2 + \frac{1}{2}\Re(Z_v(f,x))|u(f,x)|^2$. Figure 4 representing only the energy along the main bore, the darker color shading downstream of the hole location at 612 mm distance from the entrance illustrates that some of the energy is in the hole chimney. For a very specific, narrow frequency band (here around 2.3 kHz), there is no more energy in the main pipe beyond the closed side hole (position > 612 mm). This phenomenon, already observed by Petersen *et al.* (2021) has a direct influence on the acoustic impedance at the driving point.

At the junction point between the main bore and the side hole, the chimney pipe and the downstream part of the cone can be seen as two pipes in parallel, each with their own impedance $Z_{\text{chim}}(f)$ and $Z_{\text{down}}(f)$. The effective impedance is $Z_{\text{eff}} = (1/Z_{\text{chim}} + 1/Z_{\text{down}})^{-1}$. As mentioned by Chaigne and Kergomard (2016, Chap.7.7.5), it is important to include in Z_{chim} the masses of the junction (Eq. 3). At the characteristic frequency of the chimney ($f = f_{\text{chim}}$), the chimney impedance at the bore junction is very low (a pressure node), we have $Z_{\text{chim}}(f_{\text{chim}}) \ll Z_{\text{down}}(f_{\text{chim}})$. The chimney pipe can then be seen as a short circuit and $Z_{\text{eff}}(f_{\text{chim}}) \approx Z_{\text{chim}}(f_{\text{chim}})$. This can be directly observed in the input impedance (Fig. 5).

The open cone with closed chimney (see curve "Cone+Chimney", Fig. 5) behaves like an open cone without a chimney (see curve "Cone", Fig. 5, top) for most of the frequency range. Only near the characteristic chimney frequency, around 2.3 kHz (see curve "Chimney", Fig. 5), it does behave like a shortened cone, truncated and closed at the hole junction and extended by the closed chimney (see curve "Trunc. Cone + Chim", Fig. 5, bottom). The frequency range at which this phenomenon occurs is therefore only related to the length of the chimney pipe. But the value of the input impedance of the total instrument in this range depends also on the location of the hole.

This phenomenon occurs in all wind instruments with side holes. It has raised little interest so far, possibly because for most wind instruments except the bassoon the chimney lengths are small ($\ell < 7$ mm) such that the muffler effect of the closed holes occurs at frequencies $f_{\text{chim}} > 10$ kHz higher above the frequency range typically considered useful in impedance measurements (≈ 5 kHz (Le Roux *et al.*, 2008)). However, for the bassoon's particularly long chimneys (Tab. I), this phenomenon occurs at relatively low frequency (≈ 2 kHz) and its effects are clearly visible in the impedance measurement.

In Figure 6, the impedances measured on the French bassoon for the lowest fingerings are compared. As Petersen *et al.* (2021) had already noticed, above about 1.7 kHz, the input impedances of the ten fingerings from B♭1 to G♯2 are equal within the measurement accuracy (deviation < 1 dB). For these ten fingerings, all holes with chimneys longer than 20 mm are closed, as well as all other side holes located upstream of the last of these long

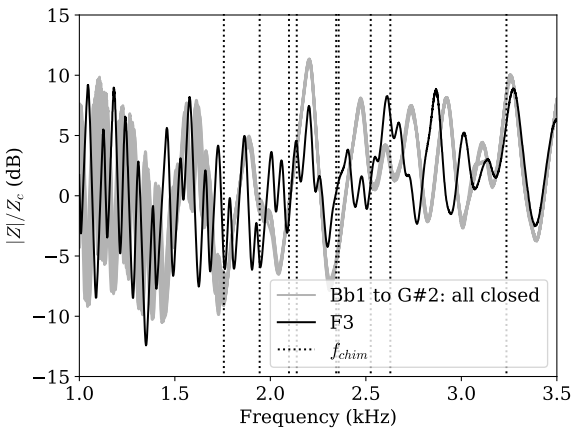

FIG. 6. Comparison of the input impedances of a French bassoon for several fingerings. Grey lines: superposition of the input impedance of the 10 lowest fingerings (B♭1 to G♯2) for which all the holes with chimney longer than 20 mm are closed. The F3 fingering for which the five longest chimneys are open (black line) has a different pattern. Vertical dashed lines: characteristic frequencies of longest chimneys (Tab. I).

holes. Therefore, in the frequency range where the muffling effect of a specific chimney occurs, the impedance of the ten finger-holes is similar to the impedance of the upstream portion of the instrument, truncated at the location of the hole under consideration, and extended by the closed chimney (as for the simplified instrument in Fig. 5). Although the effect of each long chimney is local along the frequency axis, the distribution of chimney lengths gives an overall effect, such that these 10 fingerings have the same input impedance throughout the observed range above 1.7 kHz.

For the F3 fingering, the five holes with the longest chimneys are open, including the ones placed the closest to the reed end (Tab. I). The impedance of this fingering diverges from the others in the entire range. Indeed, even at 2.36 kHz corresponding to the quarter-wave resonance of the longest closed hole for this fingering, the impedance diverges due to the difference in the upper part of the instrument.

B. Effect on the radiated sound

The evolution of the harmonic content of the sound spectrum in the room with respect to the chimney length is plotted in Figure 7 for both the conical instrument with side holes and a French bassoon. It shows both experimental data and simulations. To highlight the effect of the chimneys, the graph represents the deviation from the average magnitude of each component (see Eq. 1, Sec. II B 3).

Firstly, we discuss the simplified instrument, when the three chimneys have the same length (Fig. 7.a and b). Notches are clearly visible in the radiated sound spectra at the chimney resonance frequencies (f_{chim}, $3f_{\text{chim}}$, $5f_{\text{chim}}$, ...) both in measurement and simulation. To demonstrate this effect animated spectrograms with experimental sound data are provided as supplementary materials [2] [3]. Due to the cumulative effect of the three chimneys, when f_{chim} perfectly matches the frequency of one partial, its attenuation in the room can reach -30 dB and even -40 dB in simulated data. However, if f_{chim} is in between two partials the radiated sound is almost not altered, as for a chimney length of about 60 mm in Fig. 7.a and b. When length offsets are applied to the chimneys of this simplified instrument, a series of three notches can be observed (Fig. 7.c and d), corresponding to the characteristic frequencies of each of the chimneys. The attenuation is less pronounced (about −10 dB to −15 dB), especially for smaller chimney lengths ($\ell < 40$mm), when their effect does not overlap in the frequency domain. However, when the characteristic frequencies are sufficiently close ($\ell > 40$mm for the lowest notch), the effect of the three chimneys overlap and each partial is affected by a wider range of configurations.

The effect of matching chimney lengths on the level of the partial closest to 1.8 kHz is shown in detail in Figure 8 (left), for the two situations without (plain line) and with offsets (dashed line). For the case without offset the notch is 10 dB stronger than for the more realistic case with offset, as shown for the French bassoon in Figure 8 (right). In the simulations (grey curves), the effect is even more pronounced than in the experiment (black curves), possibly due to the absence of ambient noise in simulation. The simulation-measurement agreement is acceptable considering the geometric discrepancies and the different estimates of the radiated power (single point vs. spatial integration).

The decreasing importance of the "notch-effect" in more realistic cases becomes evident in the simulated and measured external spectra of the French bassoon. On Figure 7.e, the simulation shows how the effect is partially obscured by the geometric complexity of such instrument (open holes and bore irregularities). In the measurements, the evolution of the notches with chimney length can only be guessed (Fig. 7.f). This is still visible when it occurs at low frequency ($f < 3$ kHz, for long chimneys $\ell > 20$ mm) (e.g. Fig. 8, left). However, this pattern becomes almost invisible at high frequencies ($f > 3$ kHz, for short chimneys or higher chimney resonances).

This can partially be explained by the influence of directivity, which is present in the measurement but not in the simulations. Figure 9 shows the simulation of the power spectrum radiated by one single hole, namely the D-key hole near the boot of the instrument. The radiated power at some partials above 3 kHz strongly varies without clear correlation with the chimney length. These variations are not visible in Figure 7.e, where the total power radiated by all the holes together is plotted (Eq. 6). It suggests that the energy distribution between the openings is changed. As a consequence, the directivity of the instrument is also changed. It is important to

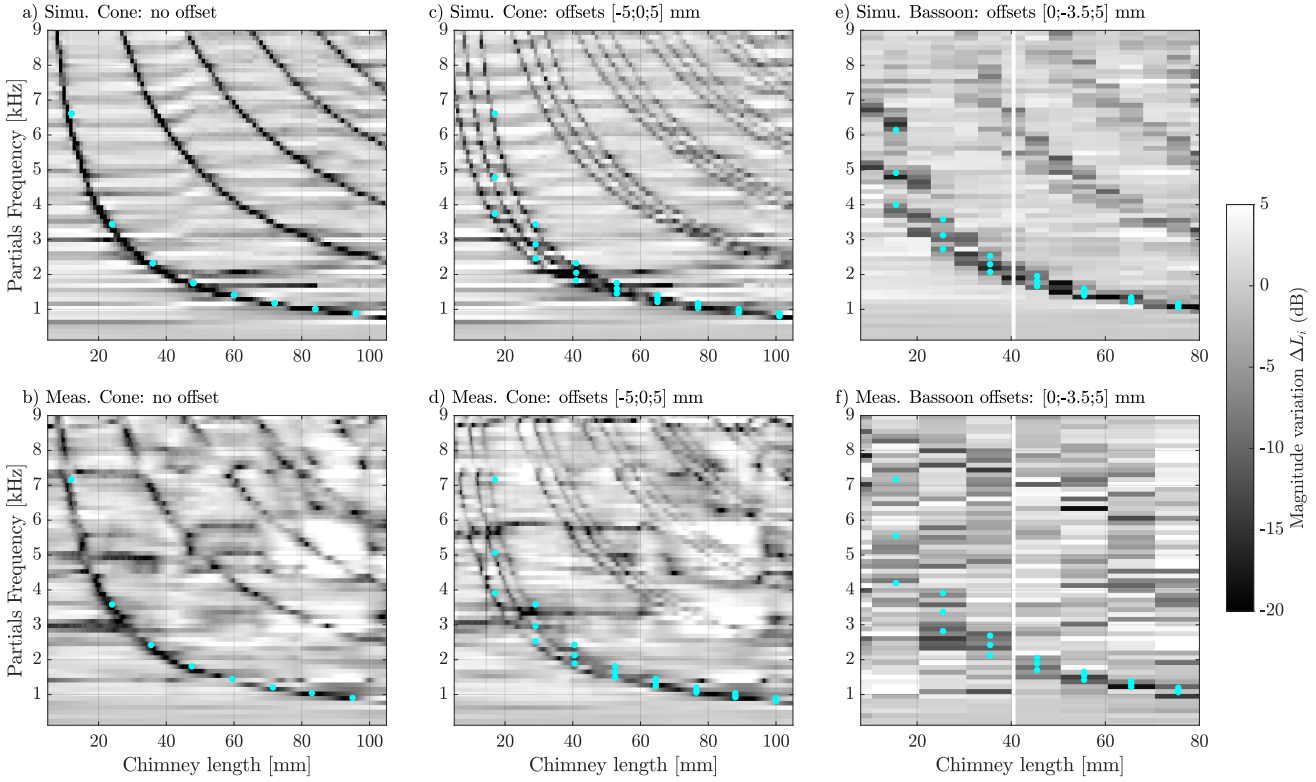

FIG. 7. Variation of the sound spectrum of note C♯3 (Cone: $f_0 \approx 130$ Hz; Bassoon: $f_0 \approx 137$ Hz), with respect to the closed chimney length. The shading represents the level in dB with respect to the mean level per partial (cropped to [-20 dB, 5 dB] for readability). First row (a, c, e) corresponds to simulations and second row (b, d, f) to measurements. (a) and (b): Cone with three closed chimneys of equal length; (c) and (d): Cone with three chimneys of different lengths; offset [-5mm, 0mm, 5mm]; (e) and (f): French bassoon fingered $C\sharp$, length of three original finger holes varied using a piston by keeping the original offset [0mm, -3.5mm, 5mm] (Tab. I). The cyan dots correspond to the characteristic frequency f_{chim} of the closed chimneys. The white vertical line in (e) and (f) indicates the regular lengths of the bassoon's chimneys (Tab. I)

note that, for the bassoon, depending on frequency, this scattering effect is stronger than the quarter wavelength effect and blurs it in experimental data. The simplified conical instrument having only one opening, this modification of the pattern does not happen.

In addition to the muffler effect, other changes in the radiated sound spectrum are visible in Fig. 7, especially for the simple instrument. For example, the partial near 3 kHz is about 15 dB lower for chimneys shorter than 30 mm than for long chimneys. This effect is present with and without chimney length offset and in both simulated and measured data (Fig. 7.a, b, c, d). Conversely, the partial near 3.3 kHz is about 5 dB louder for the short chimneys, and so on alternately for the other partials. This effect is almost absent for the bassoon (Fig. 7.e, f). These variations of the radiated spectrum can be related to the reed pressure.

C. Effect on the reed pressure

The observed variations in the radiated spectrum can have their origin in changes of the reed pressure spectrum. In this study, the considered quarter-wave resonances occur at frequencies much higher than the fundamental frequency of the sound ($f_{\text{chim}} > 1$ kHz, corresponding at least to the 7th partial). Moreover, the reed can be seen as a second order low-pass filter whose cut-off frequency is equal to $\omega_r/2\pi = 1.7$ kHz (cf. Eq.(4)). One could therefore assume that the quarter-wave resonances do not affect the coupling between the reed and the air column and has only a passive effect. To discuss this hypothesis, the spectrum of the pressure measured inside the double reed (reed pressure) and the spectrum of the simulated reed quantities (reed pressure, flow rate and reed blades distance) are studied.

Analogously to the external sound spectrum in Figure 7, the variation of the reed pressure spectrum with respect to the chimney lengths is represented in Figure 10 for both instruments and both simulated and experimental data [3] [4]. For the simple conical instrument (Fig. 10 a,

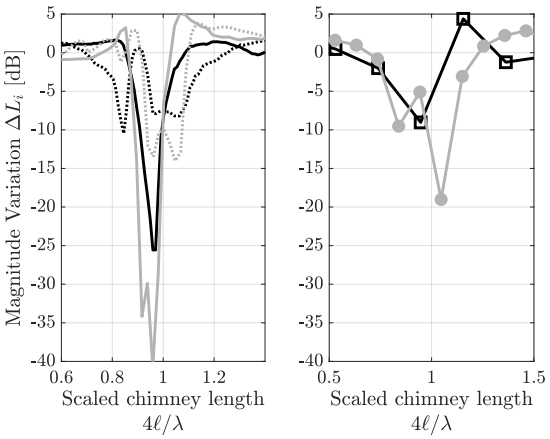

FIG. 8. Influence of the chimney length on the level of a single partial near 1.8 kHz in the external sound spectrum of the note C♯3 (Cone: $f_0 \approx 130$ Hz; Bassoon: $f_0 \approx 137$ Hz). Levels and chimney lengths are given in relative scales. Left: simple conical instrument measured (black) and simulated (gray), without (plain line) and with offsets (dashed line) between the chimneys lengths; Right: French bassoon measured (black) and simulated (gray), with offsets between chimneys lengths. For the bassoon, the chimney length step is finer for simulations than for measurements.

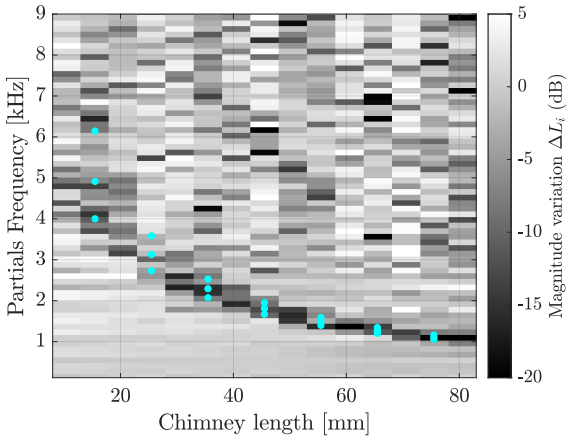

FIG. 9. Simulation of the power radiated by the D-key hole (near the boot) with respect to the chimney length. Each component is scaled by its mean magnitude.

b, c, d), variations of about ±5 dB can be observed both in simulated and measured data. As for the external sound (last paragraph of Sec. III B), the partial near 3 kHz is about 10 dB weaker for short chimneys and conversely, the partial near 3.3 kHz is about 5 dB stronger for short chimneys.

Figure 11 details the relative variation of the partial near 3 kHz of several simulated quantities for the simple instrument with chimney length offsets [-5, 0, 5] mm. The 10 dB increase in reed pressure is clearly visible. This occurs when this partial crosses the quarter-wave resonances of the chimneys (between 20 mm and 30 mm, Fig. 11, top). In addition, the input impedance is slightly higher for short chimneys (Fig. 11, top). These two variations together result in a 10 dB variation in input power: $\mathcal{P}_{in} \propto |P_{reed}|^2/\Re(Z)$ (Fig. 11, bottom). The analysis of this partial illustrates a more global redistribution of the input power along the frequency axis. Moreover, even if this partial is higher than the cutoff frequency of the reed (Tab. II), the movement of the reed follows the variation of the reed pressure. These observations suggest that the variation in reed pressure, observed in Fig. 10, is not a passive consequence of the change in impedance but results from a change in coupling between the reed and the air column. This effect is visible on the radiated power (Fig. 11, bottom) which follows the evolution of the input power ??with frequency?? except when the muffling effect occurs. In this specific configuration and for this partial, the two phenomena (change in input power and muffling effect) have similar magnitudes.

For the bassoon, this effect is less pronounced (Fig. 10.e, f). This may be a consequence of the presence of the open toneholes lattice which breaks the regularity of the impedance peaks for frequencies above about 500 Hz (Petersen *et al.*, 2021). However, in the bassoon experimental data (Fig. 10.f), strong fluctuations appear (±10 dB), apparently randomly, for frequencies above 3 kHz. Absent from the simulation data, they appear to be the result of experimental uncertainties. They could be the consequence of small fluctuations in the parameters of the artificial mouth. Indeed, as illustrated by Kergomard *et al.* (2016), the oscillation regime is very sensitive to these parameters, especially for those high partials having a relatively low magnitude compared to the lower partials (Fig. 3). These fluctuations can be related to the ones observed in the external sound (Sec. III B).

IV. DISCUSSION

The experimental setup (a simplified instrument with variable chimney lengths) and the signal processing scheme (normalization by the average spectrum) used in this study were designed especially to highlight the effect of long chimneys on the radiated sound. The effect is most clearly observed in the linear acoustic behavior of the air column, as a notch filter effect. It has consequences for the reed oscillation regime and also for the radiation. These three aspects, apparently large under laboratory conditions, are compared to other sources of sound variations in playing conditions and the perceptivity of such sound modification.

Firstly, single harmonics were found to be decreased by about 10 dB. In real musical instruments, the affected harmonics were in a much higher frequency range than the fundamental pitch. For the low register of the studied French bassoon, the lowest characteristic frequency is about 1.76 kHz (Tab. I) corresponding to the 10th partial of the note E3, and the 15th partial of the note B♭1.

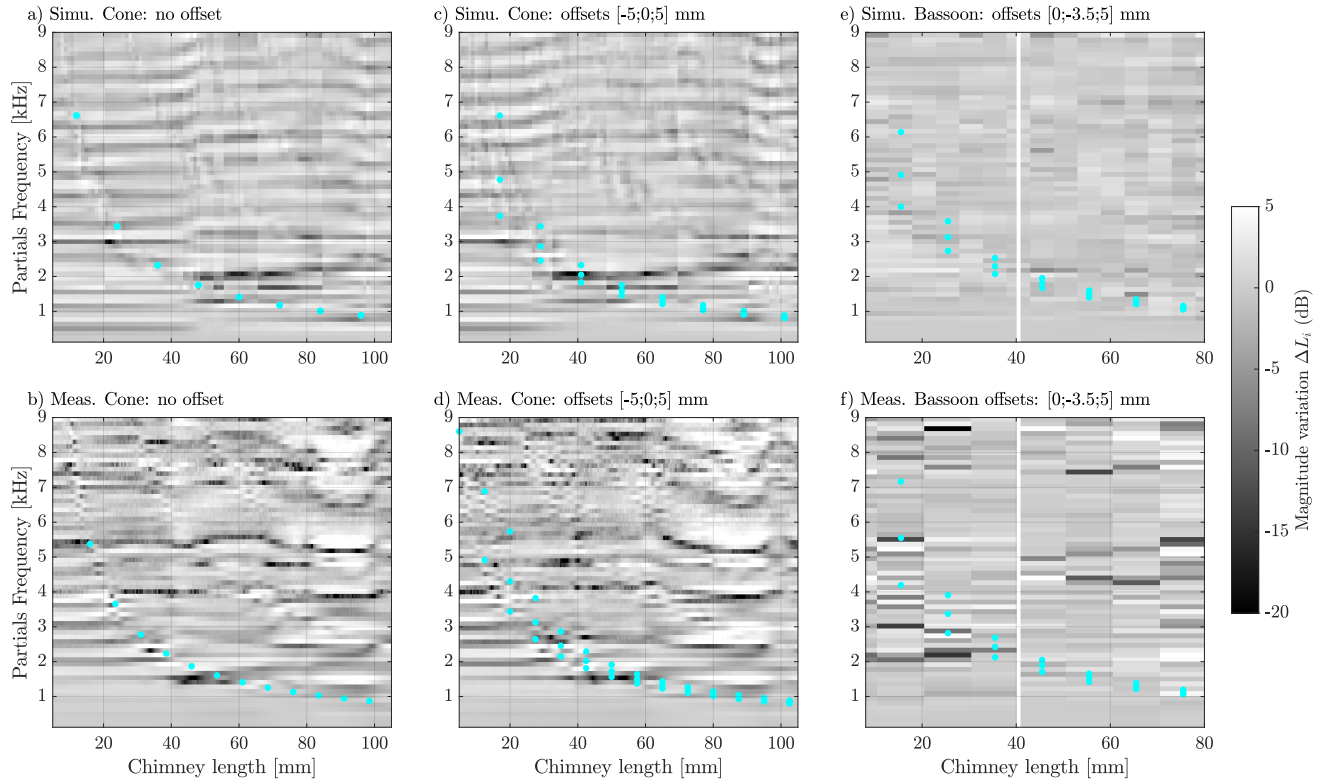

FIG. 10. Variation of the reed pressure spectrum of a played note C♯3, with respect to the closed chimney length. See caption to Fig. 7

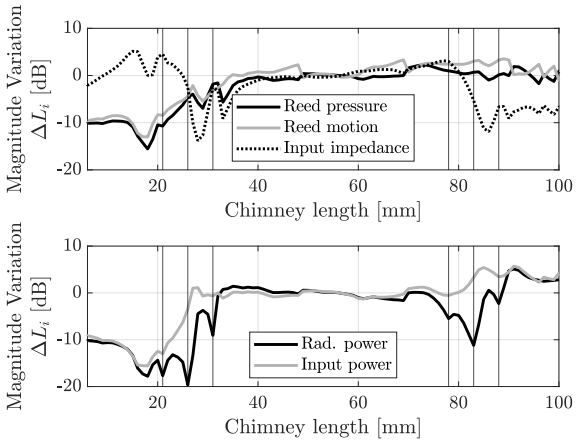

FIG. 11. Relative variation with respect to the chimney length of the spectra at the partial near 3 kHz of different simulated quantities for the cone with offsets [-5, 0, 5] mm: (top) the reed pressure, the reed motion, and the input impedance; (bottom) the input and the radiated power. The vertical lines indicate the lengths for which the quarter wavelength resonance of one chimney equals 3 kHz.

Moreover, the radiated power of these partials is low compared to the loudest partials (-10 dB, Fig. 3). The audibility of such a phenomenon is therefore not self-evident, as it can be masked by other changes in the spectrum.

Secondly, it is difficult to observe experimentally the effects of long chimneys on a real musical instrument (Section II B 2). Already a small fluctuation of the embouchure can strongly affect the spectrum at the considered frequency and making it difficult to observe the phenomenon. Even with carefully designed artificial mouth experiments, the effects are not really pronounced (Fig. 7.c). They are almost invisible on the classical absolute spectrogram, not scaled by the mean magnitude of each component, such as those presented in supplementary materials and the companion web page[3].

A third aspect is the importance of the directivity at these frequencies. The results in Section III B must be seen with the regard to the variations in the instruments directivity. For a German bassoon fingered for the note F3 it is larger than 25 dB (Grothe and Kob, 2019, 2020). Thus, the level difference between two locations in a room for a fixed chimney configuration can be larger than the level difference between two different chimney configurations at the same location.

To estimate the importance of single harmonics in the lower mid-frequency range on the overall sound perception, a preliminary study has been carried out. A

bassoon tone has been re-synthesized from the Fourier decomposition of the measured bassoon sound. This original sound is randomly compared to itself or to a modified sound in which partials 15 and 16 ($\approx$ 2 kHz) are reduced by a given level, initially set to 20 dB. After having freely played these two sounds, the test person is asked to identify whether they are similar or not. The reduction level is increased or decreased according to a "2-up 1-down" scheme, depending on the correctness of the response. It gradually converges towards the perception threshold. From a group of 22 Tonmeister[5] and music students, 10 test persons showed a converging threshold near -2.5 dB (median, range -1.5 to -6 dB), the other 12 did not show any convergence. This shows that the experimentally observed effect: a 10 dB level difference in a very narrow band of the spectrum, is only identifiable by certain trained listeners, under controlled conditions and in direct comparison. We assume that such an isolated spectrum change due to a small variation in chimney length does not dominate the perceived impression of bassoon timbre.

V. CONCLUSION

The presence of a long closed side hole affects the radiated sound of wind instruments. When the hole is closed, it induces a notch in the spectrum at a characteristic frequency corresponding to quarter wavelength of the chimney pipe ($\lambda \approx 4L$, with L the length of the chimney). More precisely, it can attenuate the radiated power of a partial by about 15 dB if the closed chimney frequency coincides with it. The effect is even larger when the air-column has several side holes with the same chimney length (Fig. 8), which is, however, rarely observed in real instruments.

The notch effect is explained by the fact that, at this frequency, the input impedance of the side branch is low. Most of the acoustic energy is deviated to the closed chimney and does not propagate into the downstream part of the instrument (Fig. 4). A consequence of this effect is also seen in the air-column's input impedance which, near this frequency, approximately equals that of an instrument rigidly terminated at the location of the side branch (Fig. 5). This affects both the source mechanism (Fig. 10), and the external sound (Fig. 7).

The notch filter has a quite narrow stop band. In our experiment on a cone at $f_0 \approx 130$ Hz the radiated sound was hardly affected if the characteristic frequency of the chimney was in between two partials. However, in a real instrument, the chimneys have different lengths and consequently a large frequency band can be affected by this phenomenon. This can readily be seen from the input impedance of the different bassoon fingerings which are all equal over the entire range above 1.7 kHz (Fig. 6), or for configurations with chimney length offset (Fig. 8).

The level of harmonic components in the resonance frequencies range of the closed chimneys, is very sensitive to both the reed excitation and the location of the listener. The sound spectrum of a woodwind instrument with many tone holes can be more different for two locations in a room than between two instruments having slightly different chimney lengths. Comparing French and German bassoon designs, the longest chimney is only 5 mm longer in the former (Nederveen, 1998). With regard to the low frequency end of the closed chimney stop band this corresponds to a shift of 300 Hz from 1.8 kHz for the French to 2.1 kHz for the German bassoon. Although an overtone level shift of a few dB in this frequency range is perceptible for trained listeners in an artificial side-by-side comparison, even a -20 dB attenuation in a narrow band with two partials seems not to change the sound color impression. However, to conclude on the effect on the global bassoon timbre a study with more ecological conditions should be conducted. A good starting point could be a comparative evaluation of blind playing experiments, in which chimney lengths can be reduced substantially in a way hidden to the player. Encompassing a series of notes and the players perspectives like intonation, playability and global timbre, it could help to understand the role of the chimney length as a possible design variable in wind instrument making.

In conclusion, while the effects of a long closed chimney on the external sound can be measured and perceived under controlled conditions, they are not predominant compared to other sources of spectrum variation (e.g., directivity). These effects may contribute to the specific sound of the bassoon, but it seems unlikely that, under normal playing conditions, the timbre difference between French and German bassoons is dominated by their long-chimneys length difference. The notch near 2 kHz observed in the spectrum in previous studies (Petersen *et al.*, 2021) (Chaigne and Kergomard, 2016, Chap.7.7.5.2) is probably more a consequence of the pressure spectrum of the reed having "natural" notches for conical instruments, than the quarter-wavelength resonance effect of a chimney.

This study also shows that a simplified model of sound generation and radiation[6] is able to predict fairly well the relative change in the external sound spectrum induced by a change in geometry (Fig. 8), even if the absolute value of this spectrum deviates from measurements (Fig. 3). Whole instrument models are not often presented in the literature and it can be emphasized that this is a further step towards computer-aided design of wind instruments.

ACKNOWLEDGMENTS

This research was supported by travel grants kindly offered by DAAD and Hochschule für Musik Detmold. We thank Zara Ali, Thomas Grosse, Malte Kob, and the Tonmeister students who contributed to this study. Stefan Pantzier provided the French bassoon, split-ball probes were provided by Diatest.

[1]The term "hole" refers to holes which are closed by the fingers, holes named "key" or "trill" are closed by pads. The "E-hole" is the one opened to go from D to E.

[2]See Supplementary materials at https://doi.org/10.1121/10.0017318. It allows listening to the modification of the external sound as a function of the chimney length for both simple instrument and bassoon.

[3] The supplementary materials are also available on the companion page: https://people.bordeaux.inria.fr/augustin.ernoult/long_chimneys

[4]See Supplementary materials at https://doi.org/10.1121/10.0017318. It allow listening to the modification of the reed pressure of both simple instrument and bassoon, as function of the chimney length.

[5]musically trained sound engineers

[6]The software Openwind (2022) is free and open access under GPL v3 license, available at https://openwind.inria.fr

Almeida, A., Vergez, C., and Caussé, R. (**2007**). "Quasi-static non-linear characteristics of double-reed instruments," The Journal of the Acoustical Society of America **121**(1), 536, http://scitation.aip.org/content/asa/journal/jasa/121/1/10.1121/1.2390668, doi: 10.1121/1.2390668.

Bilbao, S. (**2009**). "Direct Simulation of Reed Wind Instruments," Computer Music Journal **33**(4), 43–55, direct.mit.edu/comj/article/33/4/43-55/94265, doi: 10.1162/comj.2009.33.4.43.

Chaigne, A., and Kergomard, J. (**2016**). Modern Acoustics and Signal Processing *Acoustics of Musical Instruments* (Springer, New York), link.springer.com/10.1007/978-1-4939-3679-3.

Colinot, T., Guillemain, P., Vergez, C., Doc, J.-B., and Sanchez, P. (**2020**). "Multiple two-step oscillation regimes produced by the alto saxophone," The Journal of the Acoustical Society of America **147**(4), 2406–2413, asa.scitation.org/doi/10.1121/10.0001109, doi: 10.1121/10.0001109.

Colinot, T., Guillot, L., Vergez, C., Guillemain, P., Doc, J.-B., and Cochelin, B. (**2019**). "Influence of the "Ghost Reed" Simplification on the Bifurcation Diagram of a Saxophone Model," Acta Acustica united with Acustica **105**(6), 1291–1294, www.ingentaconnect.com/content/10.3813/AAA.919409, doi: 10.3813/AAA.919409.

Debut, V., Kergomard, J., and Laloë, F. (**2005**). "Analysis and optimisation of the tuning of the twelfths for a clarinet resonator," Applied Acoustics **66**(4), 365–409, linkinghub.elsevier.com/retrieve/pii/S0003682X04001276, doi: 10.1016/j.apacoust.2004.08.003.

Dickens, P., Smith, J., and Wolfe, J. (**2007**). "Improved precision in measurements of acoustic impedance spectra using resonance-free calibration loads and controlled error distribution," The Journal of the Acoustical Society of America **121**(3), 1471–1481, asa.scitation.org/doi/10.1121/1.2434764, doi: 10.1121/1.2434764.

Eddy, D. (**2016**). "Acoustic Impedance Probe for Oboes, Bassoons, and Similar Narrow- bored Wind Instruments," in *DAGA2016 - 42nd German Annual Conference on Acoustics*, Aachen, pub.dega-akustik.de/DAGA_2016/data/articles/000484.pdf.

Ernoult, A., Chabassier, J., Rodriguez, S., and Humeau, A. (**2021**). "Full waveform inversion for bore reconstruction of woodwind-like instruments," Acta Acustica hal.inria.fr/hal-03231946, doi: 10.1051/aacus/2021038.

Fabre, B., De La Cuadra, P., and Ernoult, A. (**2019**). "How do flute players adapt their control to modifications of the flute bore ?," in *International Symposium on Music Acoustics (ISMA)*, Detmold, pp. 15–20, pub.dega-akustik.de/ISMA2019/data/articles/000067.pdf.

Field, C., and Fricke, F. (**1998**). "Theory and applications of quarter-wave resonators: A prelude to their use for attenuating noise entering buildings through ventilation openings," Applied Acoustics **53**(1-3), 117–132, linkinghub.elsevier.com/retrieve/pii/S0003682X97000352, doi: 10.1016/S0003-682X(97)00035-2.

Gibiat, V., and Laloë, F. (**1990**). "Acoustical impedance measurements by the two-microphone-three-calibration (TMTC) method," The Journal of the Acoustical Society of America **88**(6), 2533–2545, asa.scitation.org/doi/10.1121/1.399975, doi: 10.1121/1.399975.

Grothe, T. (**2013**). "Experimental Investigation of Bassoon Acoustics," Ph.D. thesis, Technischen Universität Dresden, d-nb.info/1068447982/34.

Grothe, T. (**2015**). "Parameters ranges for artificial bassoon playing," in *Vienna talks*, Vienne, viennatalk2015.mdw.ac.at/proceedings/ViennaTalk2015_submission_78.pdf.

Grothe, T., and Amengual Garí, S. V. (**2019**). "Measurement of "Reed to Room"-Transfer Functions," Acta Acustica united with Acustica **105**(6), 899–903, www.ingentaconnect.com/content/10.3813/AAA.919370, doi: 10.3813/AAA.919370.

Grothe, T., and Baumgart, J. (**2015**). "Assessment of Bassoon Tuning Quality from Measurements under Playing Conditions," Acta Acustica united with Acustica **101**(2), 238–245, openurl.ingenta.com/content/xref?genre=article&issn=1610-1928&volume=101&issue=2&spage=238, doi: 10.3813/AAA.918822.

Grothe, T., and Kob, M. (**2019**). "High resolution 3D radiation measurements on the bassoon," in *International Symposium on Music Acoustics (ISMA)*, pp. 139–145, pub.dega-akustik.de/ISMA2019/data/articles/000094.pdf.

Grothe, T., and Kob, M. (**2020**). "Bassoon Directivity Data" opus.hfm-detmold.de/frontdoor/index/index/docId/97.

Kergomard, J., Guillemain, P., Sanchez, P., Vergez, C., Dalmont, J.-P., Gazengel, B., and Karkar, S. (**2019**). "Role of the Resonator Geometry on the Pressure Spectrum of Reed Conical Instruments," Acta Acustica united with Acustica **105**(2), 368–380, www.ingentaconnect.com/content/10.3813/AAA.919320, doi: 10.3813/AAA.919320.

Kergomard, J., Guillemain, P., Silva, F., and Karkar, S. (**2016**). "Idealized digital models for conical reed instruments, with focus on the internal pressure waveform," The Journal of the Acoustical Society of America **139**(2), 927–937, asa.scitation.org/doi/10.1121/1.4942185, doi: 10.1121/1.4942185.

Kergomard, J., and Heinrich, J.-M. (**1975**). "Le basson," Bulletin du GAM (82-83), www.lam.jussieu.fr/index.php?page=BulletinsGAM.

Le Roux, J. C., Dalmont, J. P., and Gazengel, B. (**2008**). "A new impedance tube for large frequency band measurement of absorbing materials," in *Acoustics 2008*, Paris, www.conforg.fr/acoustics2008/cdrom/data/articles/003579.pdf.

Lefebvre, A., and Scavone, G. P. (**2012**). "Characterization of woodwind instrument toneholes with the finite element method," The Journal of the Acoustical Society of America **131**(4), 3153–3163, asa.scitation.org/doi/abs/10.1121/1.3685481, doi: doi.org/10.1121/1.3685481.

Nederveen, C. J. (**1998**). *Acoustical aspects of woodwind instruments*, (orig. 1969) revised ed. (Northern Illinois University Press), repository.tudelft.nl/islandora/object/uuid:01b56232-d1c8-4394-902d-e5e51b9ec223.

Openwind (**2022**). "Open Wind INstrument Design" openwind.inria.fr.

Petersen, E. A., Colinot, T., Silva, F., and H.-Turcotte, V. (**2021**). "The bassoon tonehole lattice: Links between the open and closed holes and the radiated sound spectrum," The Journal of the Acoustical Society of America **150**(1), 398–409, asa.scitation.org/doi/10.1121/10.0005627, doi: 10.1121/10.0005627.

Petersen, E. A., Guillemain, P., and Jousserand, M. (**2022**). "The dual influence of the reed resonance frequency and tonehole lattice cutoff frequency on sound production and radiation of a clarinet-like instrument," The Journal of the Acoustical Society of America **151**(6), 3780–3791, asa.scitation.org/doi/10.1121/10.0011467, doi: 10.1121/10.0011467.

Pierce, A. D. (**1989**). *Acoustics: An Introduction to Its Physical Principles and Applications*, 3rd edition (2019) ed. (Springer International Publishing), link.springer.com/10.1007/978-3-030-11214-1.

Rabiner, L., and Schafer, R. (**1978**). *Digital Processing of speech signals*.

Silva, F., Guillemain, P., Kergomard, J., Mallaroni, B., and Norris, A. N. (**2009**). "Approximation formulae for the acoustic radiation impedance of a cylindrical pipe," Journal of Sound and Vibration **322**(1–2), 255–263, www.sciencedirect.com/science/article/pii/S0022460X08009085, doi: 10.1016/

j.jsv.2008.11.008.
Tang, S. K. (**2012**). "Narrow sidebranch arrays for low frequency duct noise control," The Journal of the Acoustical Society of America **132**(5), 3086–3097, asa.scitation.org/doi/10.1121/1.4756951, doi: 10.1121/1.4756951.
Thibault, A., and Chabassier, J. (**2020**). "Time-domain simulation of a dissipative reed instrument," in *Forum Acusticum*, Lyon, France, p. 6, hal.inria.fr/hal-03132474/.
Thibault, A., and Chabassier, J. (**2021**). "Dissipative time-domain one-dimensional model for viscothermal acoustic propagation in wind instruments," The Journal of the Acoustical Society of America **150**(2), 1165–1175, asa.scitation.org/doi/10.1121/10.0005537, doi: 10.1121/10.0005537.
Tournemenne, R., and Chabassier, J. (**2019**). "A comparison of a one-dimensional finite element method and the transfer matrix method for the computation of wind music instrument impedance," Acta Acustica united with Acustica **5**, 838, hal.inria.fr/hal-01963674, doi: 10.3813/AAA.919364.
Zwikker, C., and Kosten, C. W. (**1949**). *Sound absorbing materials* (Elsevier).